ACS APPLIED POLYMER MATERIALS

pubs.acs.org/acsapm Article

Adhesion of Silica and Block Copolymer Toughened Epoxy Composites

Vincent Pang, Zachary J. Thompson, Guy D. Joly, Frank S. Bates,* and Lorraine F. Francis*

Cite This: ACS Appl. Polym. Mater. 2022, 4, 6169−6178 Read Online

ACCESS | Metrics & More | Article Recommendations | Supporting Information

ABSTRACT: The effect of the size and surface functionalization of silica particle additives on the bulk and adhesive mechanical properties of neat and poly(ethylene oxide)-*b*-poly(ethylene-*alt*-propylene) block copolymer (BCP)-modified epoxies was evaluated. Three types of silica particles were investigated: microscale (diameter = 500 nm−4 μm) particles with and without phenylsilane functionalization and nanoscale particles (diameter = 140 nm) with phenylsilane functionalization. Silica particles were dispersed individually or together with block copolymers in the epoxy monomers and cured. Tensile tests revealed that the incorporation of silica increased the modulus of the composites, regardless of surface functionalization and particle size. The fracture toughness, measured by compact tension, also increased substantially when BCP was added but only modestly when each of the various silica additives was dispersed in the epoxy. Together, silica and block copolymer additives enhanced the fracture toughness, without significant effects from silica size or surface functionalization. Single-lap-joint shear tests with aluminum showed anapproximately 50% increase in adhesion strength when block copolymer micelles were dispersed in the cured epoxy, but little impact was realized from any of the silica particles studied. Failure mechanisms and the observed trends are discussed.

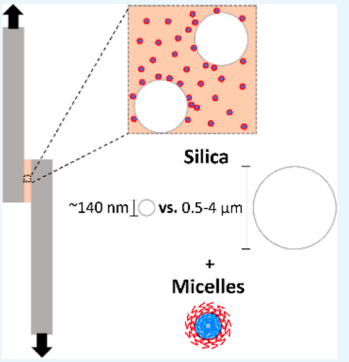

KEYWORDS: *epoxy, block copolymer, silica, adhesion, toughness, dispersion, lap-joint shear*

INTRODUCTION

Epoxies are important materials found in many industrial and consumer products. For example, thermoset epoxies are exploited as encapsulants for electronics, as the matrix material for fiber-reinforced composites, and are employed as adhesives in a host of structural applications, such as in automobiles and aircraft.[1−3] Epoxies are preferred in these applications due to their high specific strength and modulus, high glass transition temperatures, and chemical and thermal resistance.[1,3] However, these cross-linked materials generally exhibit poor fracture toughness, impacting performance in applications where fracture resistance is essential, such as in adhesives.[1,4] To overcome this limitation, efforts have been directed at improving the fracture toughness of epoxies through the introduction of various types of additives, including rubbery[4−8] and rigid particles.[9−18] This approach faces challenges associated with poor dispersion and degradation of other properties such as reductions in the elastic modulus and glass transition temperature. Block copolymer modifiers, on the other hand, have demonstrated up to 20-fold improvement in the strain energy release rate (G_{Ic}) at relatively low concentrations (<5 wt %),[19−27] which minimizes, and often eliminates, losses in modulus, strength, and glass transition temperature.

Substantial toughening from block copolymers stems from the self-assembly into nanoscale micelles when dispersed in the uncured epoxy resin. A commonly studied morphology is the spherical micelle, where an epoxy-phobic block forms the core and an epoxy-philic block promotes dispersion as the corona of the micelles.[25,28−30] These BCP micelles are kinetically trapped upon curing, rendering a glassy epoxy material.[28,31] In the case that the epoxy-phobic core block is rubbery at the use temperature, a critical amount of volumetric strain energy, associated with the stress field ahead of a crack tip due to an external load, can induce cavitation of the micelle cores.[29,32,33] Cavitated micelles behave as scattered voids, facilitating matrix yielding by reducing the critical yield stress and therefore enhancing energy dissipation of the matrix and the overall fracture toughness of the composite.[29,34]

To access further enhancements in toughening, there has been a recent push to investigate epoxy composites modified with both rigid particles and rubber/block copolymer additives.[9,35−41] Li et al. demonstrated synergistic toughening in micron-scale exfoliated graphene oxide and block copolymer-modified epoxies.[37] We have also recently demonstrated additive toughening from the addition of both block copolymer and nanosilica modifiers in epoxies.[42] This

Received: June 4, 2022
Accepted: July 12, 2022
Published: July 25, 2022

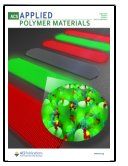

https://doi.org/10.1021/acsapm.2c00948
ACS Appl. Polym. Mater. 2022, 4, 6169−6178

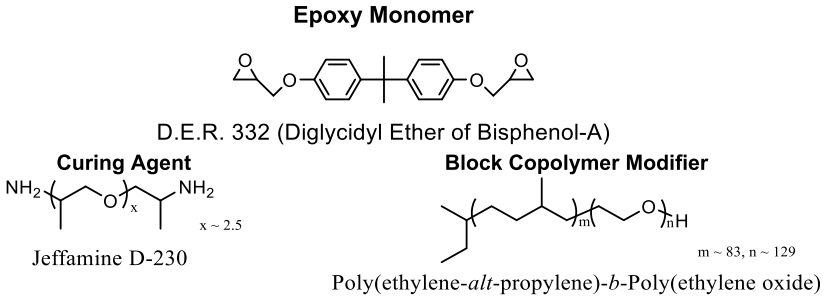

Figure 1. Chemical structures of epoxy system and block copolymer modifier.

combined toughening was shown to increase with increasing nanosilica concentration, and the elastic modulus was also shown to increase with the introduction of nanosilica additives to BCP-toughened epoxy composites. An open question from this work is whether similar improvements occur in epoxies modified with micro-sized silica particles, as these particles offer potential advantages, such as lower costs and easier processing (handling and dispersibility), over nanoparticles.

In addition to the bulk tensile and fracture properties, adhesion strength is also a critical property for epoxy adhesives. In an earlier work, we showed that BCP can significantly improve the adhesion strength of epoxies by enhancing energy dissipation in the material.[19] Other studies claim that adding rigid silica particles can also improve the adhesion strength of epoxy-based adhesives through facilitated deformation mechanisms that can dissipate energy.[43−46] However, little work has been performed to understand how adding both rigid fillers and rubbery additives, such as block copolymers, can impact the adhesion strength of an epoxy adhesive.[47] A recent paper shows that the addition of alumina particles and block copolymers to phenolic-modified epoxies has promise.[48]

In this paper, the performance of epoxy structural adhesives, modified with both BCPs and rigid silica particles of two different sizes, is explored. The bulk tensile, fracture, and adhesive properties of these composites were characterized by tensile, compact tension, and single-lap-joint shear testing, respectively. To the authors' knowledge, this is the first study to explore the impact of both block copolymers and silica particles on the adhesive properties of epoxy composites.

EXPERIMENTAL SECTION

Materials. Two reactive components were used in the epoxy formulation. Stoichiometric amounts of DER 332 (Digylcidyl Ether of Bisphenol A) epoxy monomer and Jeffamine D-230 curing agent were used as the epoxy matrix material. Chemical structures of these components are illustrated in Figure 1. The epoxy cures by step growth polymerization as the amine groups of the curing agent react with the epoxide units of the epoxy monomer, forming a crosslinks.[49]

A poly(ethylene oxide)-*b*-poly(ethylene-*alt*-propylene) (PEO-PEP or OP) diblock copolymer was dispersed in the epoxy resin as the modifier. PEP is thermodynamically incompatible with the epoxy resin and has a low glass transition temperature (T_g = −60 °C), while PEO is miscible with the epoxy resin. As demonstrated in previous publications,[22,27,42] PEO-PEP containing around 50 wt % of PEO forms relatively monodispersed spherical micelles with PEP cores when blended with a stoichiometric mixture of the epoxy and curing agent shown in Figure 1, and the micelles remain well dispersed in the cured plastic.

A batch of OP diblock copolymer was synthesized according to procedures described elsewhere.[42] Molecular weights of the individual PEP and PEO blocks were determined by H NMR. The overall molecular weight of the diblock copolymer is M_n = 11.5 kg/mol, with 5.8 kg/mol of PEP and 5.7 kg/mol of PEO. These molecular weights correspond to a virtually symmetric diblock copolymer, with a PEO weight fraction of 0.49. The dispersity of OP was determined to be 1.12 by size exclusion chromatography with room temperature tetrahydrofuran as the eluent and a refractive index detector.

Three types of silica particles were dispersed in the epoxy resin. All silica particles were provided pre-dispersed in DER 332 by 3M with ∼45 wt % loading. Two sizes were evaluated: ∼140 nm diameter nanoparticles and ∼0.5−4 μm diameter microparticles. Batches of these pre-dispersed nanoparticles and microparticles were obtained from 3M surface functionalized with phenylsilane, along with a batch of pre-dispersed non-functionalized microparticles (i.e., the surfaces contained silanol and siloxane groups). Schematics of these surface functional groups are provided in the Supporting Information (Figure S1). Surface functionalization is required to disperse the nanoparticles in DER 332; hence, non-functionalized nanoparticles were not included in this study. The nanosilica was synthesized and functionalized at 3M and the microsilica (SP60-10, Nippon Steel Corporation) was sourced by 3M and functionalized or left unfunctionalized prior to dispersion in DER 332. The microsilica particle size distribution, analyzed by SEM, is shown in Figure S2.

Epoxy Preparation and Dispersion. Resin/additive mixtures were first prepared by mixing OP with the stock mixture of pre-dispersed silica particles and epoxy monomer at elevated temperatures (70−80 °C) without solvent for 2−3 days. Target concentrations of 5 wt % OP and 10 wt % silica in the final dispersions containing either or both additives were achieved by diluting the pre-dispersed silica stock mixture with additional DER 332 and a specified amount of diblock copolymer.

Once the additives and epoxy resin were homogeneously mixed, Jeffamine D-230 was added to the mixture and stirred at 60 °C for 40 min, while actively pulling vacuum to degas. The formulation was then poured into rectangular molds or spread onto aluminum sheets for curing. The rectangular molds yielded plaques that were machined into bulk tensile or compact tension specimens. Bonded aluminum sheets were used to prepare single lap joints for adhesion testing. The curing cycle included a 2 h cure at 80 °C, followed by a 4 h post-cure at 125 °C. The cured epoxies were then slowly cooled to room temperature. This procedure fully cures the epoxy resin, as shown in our previous work.[42]

Transmission electron microscopy (TEM) was performed to characterize the dispersion of the silica particles using an FEI Tecnai T12 Transmission Electron Microscope with a 120 kV accelerating voltage. The dispersion of particles near the epoxy/aluminum interface was also characterized with TEM. Droplets of the uncured composite resins were placed on the aluminum substrates prepared by the same cleaning process described for single lap joints and then cured under the same conditions as the lap shear joints. The cured composites were removed by cryogenically chilling with liquid nitrogen, and then encased in an embedding resin and sectioned and prepared for characterization by TEM. Details of the embedding, sectioning, staining, and imaging are described elsewhere.[19,42]

Challenges were encountered when cross-sectioning and imaging specimens containing microsilica particles. Due to the large size of the particles compared to the 70−100 nm thick sections, the obtained sections typically have large holes and inconsistent section

https://doi.org/10.1021/acsapm.2c00948
ACS Appl. Polym. Mater. 2022, 4, 6169−6178

thicknesses. The defects in these sections limit the magnification and area of the sample that can be imaged. Thus, the images shown are only of areas that are intact, typically with smaller silica particles, and at magnifications that do not resolve the micelles. In addition, a lack of staining contrast limited direct observation of the micelles by TEM, possibly due to an unoptimized staining procedure for this specific block copolymer. However, small angle X-ray scattering data of OP in the epoxy system studied here were reported in a previous study and provide evidence of OP micelles, with an average core diameter of 21 nm.[42]

Bulk Tensile Properties. Yield strength and elastic modulus were characterized with tensile and compact tension testing. Tensile tests were performed using "dogbone" specimens following ASTM D-638 with a "Type V" specimen geometry (Figure S3).[50] Testing was performed using an Instron 5966 Universal Testing System equipped with a 10 kN load cell, wedge action tensile grips, and an AutoX extensometer. Load and strain (extension) measurements were obtained at room temperature with a 10 mm/min crosshead displacement rate.

Compact tension testing was conducted with specimens following ASTM D-5045.[51] Details of the specimen geometry are described in the Supporting Information (Figure S4). Testing was done on an Instron 5966 Universal Testing System with a 500 N load cell and custom compact tension grips. Load and displacement data were obtained at room temperature with a 10 mm/min crosshead displacement. Specimen preparation details are described elsewhere.[42]

Adhesion Strength. Adhesion strength was measured by single-lap-joint shear tests following ASTM D-1002.[52] The single lap joints consisted of two 2024 T3 aluminum adherends bonded with the epoxy formulations over an overlap area (Figure S5) with a bondline thickness of ~0.1 mm (Table S2). This constant thickness is the same as that used in our previous work[19] and allows for comparison without interference from thickness variation effects.[2,53] Details of overlap dimensions and substrate roughness are described elsewhere.[19] Residual grit was removed from the aluminum surfaces by repeated acetone and isopropanol rinses, with wiping until grit is no longer seen visually. The loads during these tests were well below the yield strength of the 2024 T3 aluminum.[54] The Instron 5966 Universal Testing System was also used for these measurements at room temperature and a 1.3 mm/min crosshead displacement, yielding load and displacement measurements.

Fracture Surface Imaging. The fracture surfaces of compact tension specimens and adhesive failure surfaces of single lap joints were imaged with scanning electron microscopy. In both cases, the specimens were fixed on aluminum stubs with conductive carbon tape. The surfaces were coated with a 2 nm thick layer of iridium to reduce charging in the SEM. A Hitachi SU-8230 Scanning Electron Microscope was used to characterize the surfaces, using a 5 kV accelerating voltage, 5 μA emission current, 6 mm working distance, and both upper and lower secondary electron detectors.

RESULTS AND DISCUSSION

Composite Microstructure. Dispersion of the microsilica particles in the cured epoxy was characterized by TEM. Functionalized and non-functionalized versions of these particles were well-dispersed with no agglomeration in the cured composites without the block copolymer as shown in Figure 2a,c. Addition of 5 wt % block copolymer did not influence the dispersion, as illustrated in Figure 2b,d. This result contrasts with our previous work showing partial aggregation of the surface-functionalized nanosilica particles in the presence of BCP.[42] Aggregation of nanosilica particles was attributed to attractive depletion and bridging forces associated with micelles near and adsorbed onto the functionalized silica surfaces.[42]

The improved dispersion of microsilica particles in the presence of BCP micelles may be due to a change in the depletion potential with the onset of "depletion stabilization",

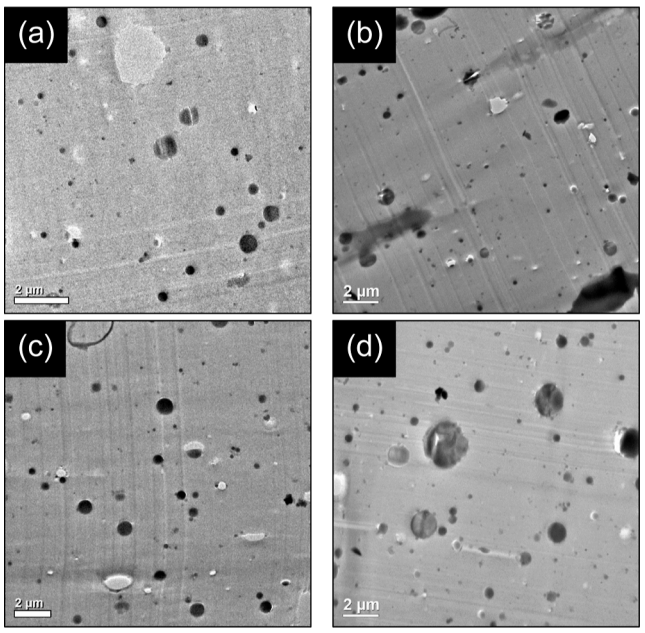

Figure 2. TEM images of cured composites containing silica with and without the block copolymer: (a) 10 wt % functionalized microsilica; (b) 10 wt % functionalized microsilica and 5 wt % OP; (c) 10 wt % non-functionalized microsilica; and (d) 10 wt % non-functionalized microsilica and 5 wt % OP.

that is, an increase in a structural energy barrier with an increase in the particle size ratio $d_{silica}/d_{micelle}$.[55−59] The particle size ratio increases from 7 (for 140 nm diameter nanosilica) to about 50 (for a 1 μm diameter microsilica particle) (Figure S2), while the micelle core diameter is maintained at 21 nm.[42] One aspect of depletion stabilization is that the attractive depletion well depth increases with increased particle size ratio, resulting in a stronger short-range attractive potential.[55,58] However, a structural energy barrier[55−59] also forms as layers of the more numerous, smaller micelles block the silica particles from approaching each other in the uncured resin. This structural energy barrier grows larger for larger size ratios.[55] We suspect that the thermal motion of the microsilica colloids in the unreacted epoxy resin is not enough to overcome the structural energy barrier, resulting in little or no aggregation. Additionally, this barrier against short-range interactions impedes any aggregation mechanisms that could be operative due to micelle adsorption, resulting in no difference in dispersion with surface functionalization.

Functionalization, however, appears to impact the organization of micelles near the microsilica particles. While not apparent in TEM, a difference in the micelle adsorption behavior is observed on the fracture surfaces of functionalized and non-functionalized microsilica-modified epoxies (Figure 3). Figure 3a shows an array of cavities lining the pulled-out functionalized silica particle pits, whereas Figure 3b shows featureless pulled-out non-functionalized silica particle pits. These features suggest BCP micelle adsorption on functionalized microsilica but not on non-functionalized microsilica (details in the Supporting Information). As described in a previous work, the PEO blocks of the micelles prefer to interact with the functionalized nanosilica based on the surface energies.[42] As shown in the next section, the mechanical properties of the composites studied here are not significantly affected by functionalization and micelle adsorption behavior.

https://doi.org/10.1021/acsapm.2c00948
ACS Appl. Polym. Mater. 2022, 4, 6169−6178

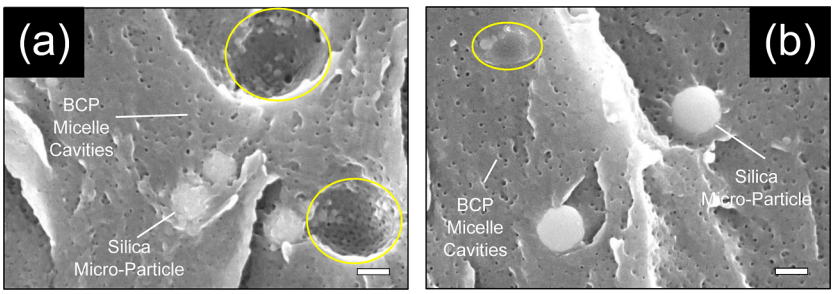

Figure 3. High magnification SEM micrographs of the fracture surfaces of compact tension specimens containing silica with and without block copolymers: (a) 10 wt % functionalized microsilica and 5 wt % OP; (b) 10 wt % non-functionalized microsilica and 5 wt % OP. Pits from pulled-out microparticles are highlighted in yellow. Scale bars are 200 nm long.

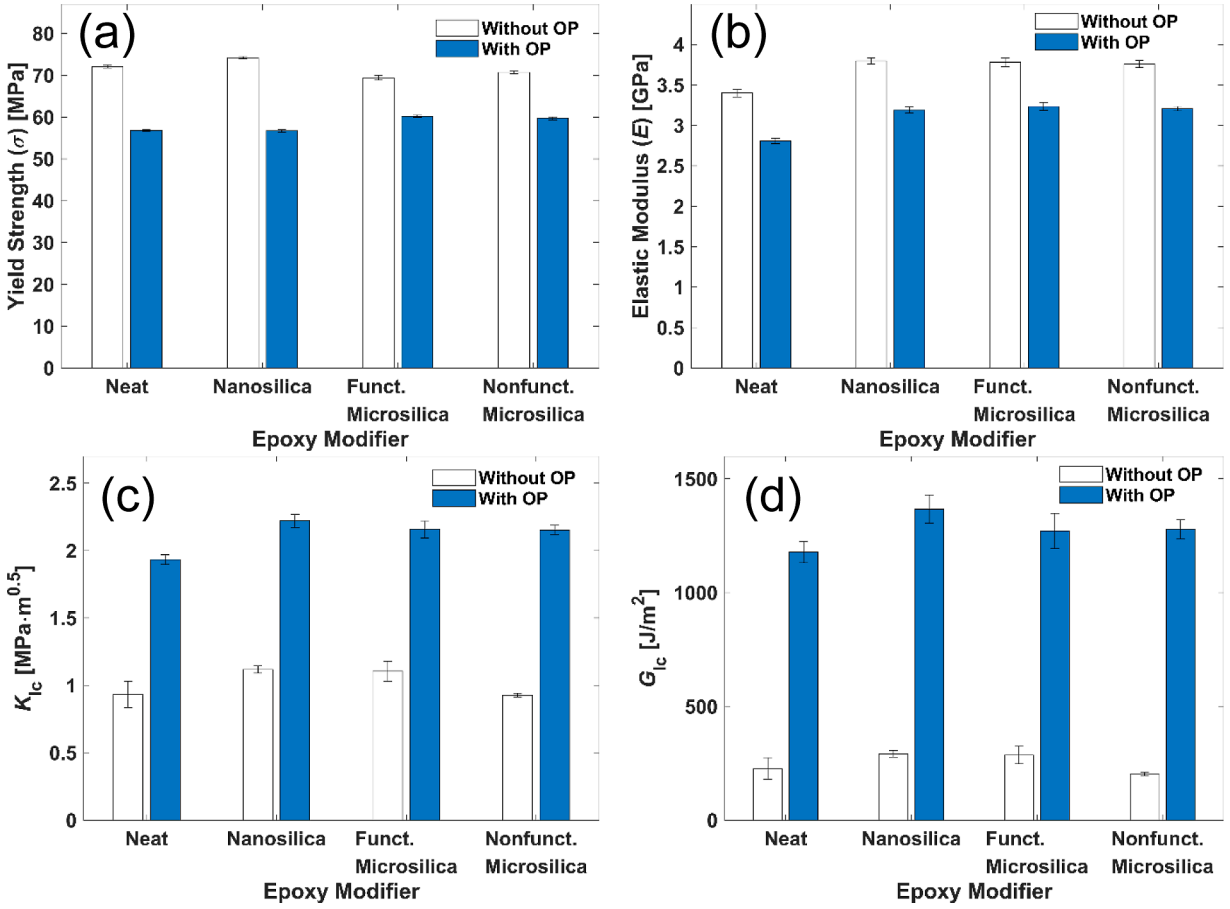

Figure 4. Bar graphs of (a) yield strength, (b) elastic modulus, and (c) K_{Ic} and (d) G_{Ic} as functionalization and particle size are varied. Nanosilica data are adapted from [42].

Tensile and Fracture Properties. Yield strength, elastic modulus, and fracture toughness (K_{Ic} and G_{Ic}) were determined by tensile and compact tension testing of bulk epoxy composites with 5 wt % OP and 10 wt % of each type of silica. A comparison of these properties is shown in Figure 4. The results were extracted from tensile test stress versus strain plots (Figure S6) and compact tension load versus displacement plots (Figure S7). Strain energy release rate, G_{Ic}, was calculated with eq 1 and the plane strain fracture toughness, K_{Ic} (Figure 4c), and elastic modulus (Figure 4a) results, assuming a Poisson's ratio, ν, of 0.34.[60] The same ν is assumed in samples with incorporated additives due to their relatively low concentrations.

$$G_{Ic} = \frac{K_{Ic}^2}{E}(1 - \nu^2) \quad (1)$$

Overall, Figure 4 shows that strength, modulus, and fracture toughness properties of the microsilica-modified epoxies are similar to those of nanosilica-modified epoxies, which have been described previously.[42] In brief, the addition of block copolymer (OP) reduces the overall yield strength and modulus of the composite, whereas the addition of the silica particles studied here increases the modulus, with no significant effect on strength. The modulus of the composites containing 10 wt % silica particles is between the Voigt and Reuss bounds and is similar to those in other works.[17,61] See the Supporting Information. The moduli of composites

https://doi.org/10.1021/acsapm.2c00948
ACS Appl. Polym. Mater. 2022, 4, 6169−6178

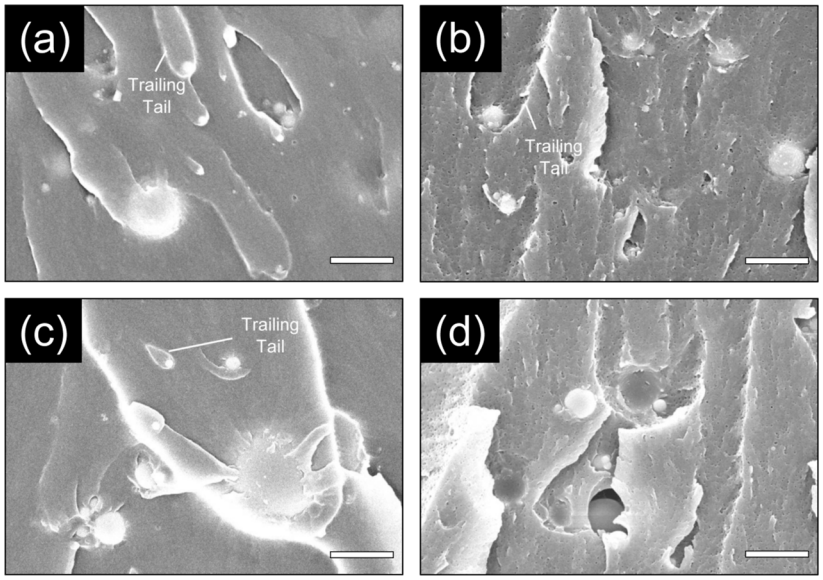

Figure 5. SEM micrographs of the fracture surfaces of compact tension specimens containing silica with and without block copolymers: (a) 10 wt % functionalized microsilica; (b) 10 wt % functionalized microsilica and 5 wt % OP; (c) 10 wt % non-functionalized microsilica; (d) 10 wt % non-functionalized microsilica and 5 wt % OP. Scale bars are 1 μm long. (c) and (d) are lower magnification images of the same surfaces as in Figure 3.

containing silica microparticles are the same as those containing silica nanoparticles within experimental error. Our past work showed that the increase in modulus of composites containing nanosilica over 5−25 wt % follows the Mori−Tanaka model.[13,62] Adding the silica particles led to modest improvements in K_{Ic} and G_{Ic}, whereas adding block copolymers led to significant enhancements to the fracture toughness. When both BCP and silica are added together, some of the modulus loss from the BCP addition is recovered, and K_{Ic} and G_{Ic} are increased beyond the toughening achieved by the additives individually.

The similar impacts on yield strength from the various silica particles may be due to the matrix−particle interactions that are present in these composites and the relatively low concentrations of silica studied here. We have shown previously that the functionalized nanosilica has an intermediate particle−matrix interfacial strength, resulting in no significant effect on strength.[42] The particle size change with the functionalized microsilica is not expected to change the interfacial adhesion and therefore the impact on strength. Functionalized and non-functionalized microsilica particles may both also rely on weak intermolecular interactions for interfacial bonding, leading to similar effects on strength. Additionally, the particle concentration may not be high enough to resolve any trends in strength from the difference in particle functionalization.

There is no change in modulus enhancement from varying size and functionalization. These parameters have little impact on modulus, which primarily depends on concentration and moduli of the composite components.[13] Functionalization and particle size primarily affect surface interactions, which play only a minor role due to the low extent of stress in the linear elastic regime, where elastic modulus is measured.[13]

The toughening behavior is also consistent across all types of silica, regardless of size and functionalization. Surprisingly, the microparticles perform nearly as well as the nanoparticles and do not require functionalization for dispersion or performance. Silica size would primarily impact the silica toughening mechanisms that are operative, but these mechanisms are generally not as effective as cavitation of rubber additives.[9] The mechanisms leading to the modest toughening with silica and significant toughening with block copolymers are revealed through features on the fracture surfaces shown in Figure 5. Low magnification images of the surfaces shown in Figure 5 are in the Supporting Information (Figure S8).

In the images with functionalized microsilica (Figure 5a,b) and non-functionalized microsilica (Figure 5c,d), crack pinning and deflection appear to be the cause for the observed modest toughening.[9,40,63,64] The residual tails trailing behind particles as the crack front moves are characteristic of bowing of a crack front, likely due to crack pinning and deflection.[64] Crack pinning and deflection expose more matrix material to the crack tip stress field and expand the volume of material that undergoes yielding. In contrast, debonding and void growth are the primary mechanisms leading to the modest toughening from nanosilica, as shown by previous works.[9,17,38,61] Although the operative mechanisms for silica particles change with particle size, they all lead to similar modest amounts of toughening (Figure 4) found in this study.

There is significant toughening from OP micelles in the microsilica-based composites as in those with nanosilica. Without block copolymers (Figure 5a,c), the fracture surface is featureless in the area between the silica particles. In specimens with block copolymers (Figure 5b,d), cavities of size similar to the block copolymer micelles are dispersed across the fracture surface (see also Figure 3 for high magnification fracture surface images). We interpret these features to be remnants of the cavitation and facilitated yielding mechanism, leading to the substantial measured toughening.[32−34,65] In the specimens with both additives, features owing to the mechanisms associated with both silica and OP are present. This suggests that the combined toughening with the hard and soft particles is due to the individual toughening mechanisms occurring in tandem, without disruption of either.

Adhesion Strength. Adhesion strengths of the neat and 5 wt % OP modified epoxy materials, further modified with the various types of silica, were measured by single-lap-joint shear testing at a constant adhesive thickness. This test resulted in

https://doi.org/10.1021/acsapm.2c00948
ACS Appl. Polym. Mater. 2022, 4, 6169−6178

shear stress versus extension measurements (Figures. S9 and S10) that were used to determine adhesion strength. The adhesion strengths, shown in Figure 6, were determined from the maximum shear stress, which typically occurs at the point of joint failure.

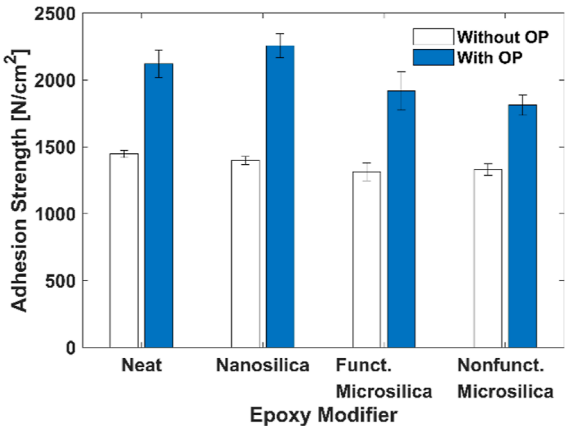

Figure 6. Bar graph of single-lap-joint shear adhesion strengths as functionalization and particle size (nanosilica vs microsilica) are varied.

The trends in adhesion strength follow closely with the associated fracture toughness. Adding block copolymer micelles significantly increases the adhesion strength of the epoxy adhesives, consistent with our previous study on BCP-modified epoxy adhesives prepared without silica.[19] When loading these joints, there are not only primary shear stresses but also transverse normal stresses due to bending moments that arise from the eccentric loading path of the single lap joint.[3,66] Hence, adhesive failure does not occur in pure shear. The normal stresses lead to hydrostatic stresses near the crack tip that can be great enough to induce cavitation and enhance the local energy dissipation within the adhesive, improving the adhesion strength.[19]

The adhesion strength of the neat epoxy adhesive is not affected by silica size and functionalization. This differs from the trends seen with composites that also include OP; nanosilica slightly improves and microsilica slightly reduces the adhesion strength of the OP-modified epoxy. These minor effects from added silica on the adhesion strength of modified epoxies can be further explored by investigating the interfacial failure behavior of these specimens, as discussed below.

Surfaces of the failed adhesives imaged by SEM are shown in Figure 7. The features from these micrographs are similar to those shown on the bulk compact tension fracture surfaces (Figure 5). The failure surfaces of the adhesives modified by silica alone (Figure 7a,c,e) show features that correspond to the mechanisms that are operative in bulk tensile failure (see Figure 5a,c for fracture surface SEM images of specimens containing microsilica and ref 42 for specimens containing nanosilica).[42] The spherical-cap pits of Figure 7a suggest debonding and void growth of the nanosilica and the tails

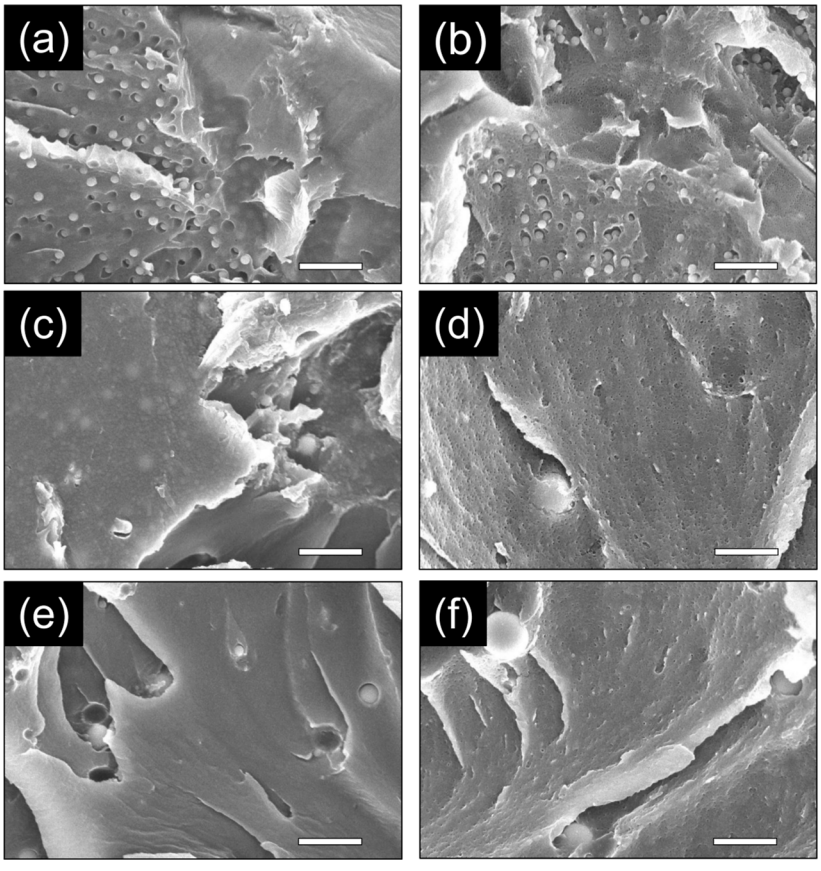

Figure 7. SEM micrographs of the single-lap-joint failure surfaces of specimens containing silica with and without block copolymers: (a) 10 wt % nanosilica; (b) 10 wt % nanosilica and 5 wt % OP; (c) 10 wt % functionalized microsilica; (d) 10 wt % functionalized microsilica and 5 wt % OP; (e) 10 wt % non-functionalized microsilica; (f) 10 wt % non-functionalized microsilica and 5 wt % OP. Scale bars are 1 μm long.

https://doi.org/10.1021/acsapm.2c00948
ACS Appl. Polym. Mater. 2022, 4, 6169−6178

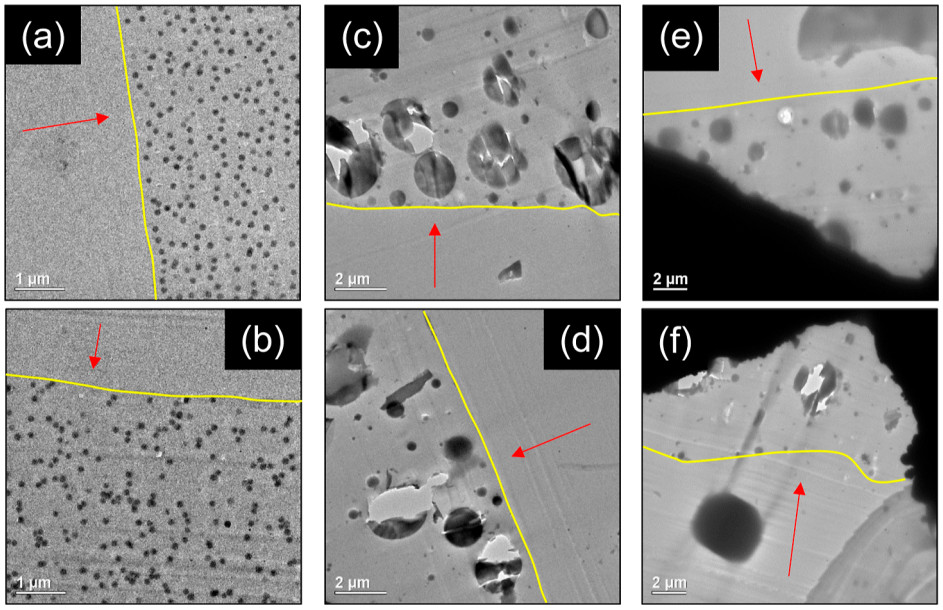

Figure 8. TEM images of the interface between aluminum and cured composites containing silica with and without block copolymer: (a) 10 wt % nanosilica; (b) 10 wt % nanosilica and 5 wt % OP; (c) 10 wt % functionalized microsilica; (d) 10 wt % functionalized microsilica and 5 wt % OP; (e) 10 wt % non-functionalized microsilica; (f) 10 wt % non-functionalized microsilica and 5 wt % OP. The yellow lines mark the original interface between the composite and aluminum, and the red arrows point from within the embedding resin (where the aluminum was) to the interface. The TEM sample grid and some debris are present in (e) and (f).

found in Figure 7c,e suggest crack deflection around the microsilica. On the failure surfaces of adhesives with both block copolymer and silica (Figure 7b,d,f), the same features from the silica are present, along with small cavities scattered across the surface. This suggests that the cavitation mechanism plays a significant role in enhancing energy dissipation, even in the presence of dispersed silica particles. Additionally, micelle cavities in pulled-out silica pits and extracted micelles on remnant functionalized silica particles (Figure 7d) provide further evidence of favorable interactions between micelles and the phenylsilane-functionalized silica particles but not with non-functionalized silica particles (Figure 7f).

Although similar features appear on both the adhesive failure (Figure 7) and bulk fracture surfaces (Figure 5) of epoxies modified with silica, the silica particles lead to only minor or no changes in adhesion strength (Figure 6). The toughening mechanisms attributed to these particles may only be contributing an insignificant effect on the measured adhesion strength. One possibility is that the energy dissipation contributions from these particles may also be redundant with mechanical interlocking effects from the roughened substrate.[67,68] As a crack progresses along the adhesive–adherend interface, the roughness of the substrate causes the crack to either deflect, analogously to microsilica crack deflection, or progress into the adhesive material for cohesive failure. Photographs of the failure surfaces in Figures S11 and S12 show mixed adhesive and cohesive mode failure, consistent with our previous work,[19] and support this effect from mechanical interlocking.

The organization of silica particles near the aluminum–epoxy interface of the adhesive joints for the various cured composites is shown in Figure 8. In all cases, the dispersion of silica particles is the same as that seen in the bulk of the adhesive, that is, away from the interface (see Figure 2). In all cases, with BCP (Figure 8b,d,f) and without BCP (Figure 8a,c,e), there is no aggregation of silica particles at the aluminum interface. This behavior suggests that both functionalized and non-functionalized microsilica particles have no preference for interactions with the aluminum surface. PEP-PEO (i.e., OP) block copolymer micelles have also been previously shown to have no preference for interacting with the aluminum surface.[19] Therefore, these additives primarily impact the adhesion strength results through the enhancement of local energy dissipation, with little contribution to the interfacial bonding.

Finally, the significant improvement in adhesion strength from block copolymer micelles is mostly maintained (within 15% of that of the OP-modified epoxy adhesive) when also incorporating any of the silica additives. As shown in Figure 6, small differences in adhesion performance between the nanosilica versus microsilica in OP-modified epoxies appear to exist. However, we are unable to determine the origins of these differences with the limited scope of the results reported here. These trends may be further explored (e.g., with different substrate surface material and priming and with different adhesive thicknesses and varying silica concentration) in future studies. Overall, these results show that the addition of silica particles to block copolymer-modified epoxies provides a way to improve other properties, such as modulus, without jeopardizing adhesion strength.

CONCLUSIONS

Phenylsilane surface-functionalized silica nanoparticles, functionalized and non-functionalized (siloxane and silanol surface groups) silica microparticles, and a poly(ethylene oxide)-*b*-poly(ethylene-*alt*-propylene) (OP) diblock copolymer were blended with bisphenol A diglycidyl ether and with a Jeffamine hardener and reacted at elevated temperature. The impacts of these additives on the mechanical and adhesive properties of the cured formulations were studied. The OP diblock copolymer forms well-dispersed spherical micelles in the cross-linked epoxy. Functionalized nanosilica, functionalized

https://doi.org/10.1021/acsapm.2c00948
ACS Appl. Polym. Mater. 2022, 4, 6169−6178

microsilica (500 nm−5 μm diameter), and non-functionalized microsilica were individually dispersed in the epoxy resin and all formed stable dispersions.

As measured by compact tension experiments, fracture toughness, K_{Ic} and G_{1c}, of the epoxy, was enhanced by each additive. Individually, 5 wt % OP and 10 wt % silica increased K_{Ic} by 100 and 20%, respectively. This toughening was consistent across all types of silica additives, regardless of particle size and surface functionalization. Together, the combined toughening was additive, with a 120% increase to K_{Ic}. Toughening mechanisms associated with silica and OP operate simultaneously, and without mutual disruption, leading to combined toughening.

Addition of block copolymer micelles to the glassy epoxy increased the single-lap-joint shear adhesion strength by approximately 50%. The adhesion strength was essentially unaffected by the presence of any of the silica particle additives under the conditions selected in this study, and the improvements in adhesion strength from the micelles were mostly maintained (within 15% of that with neat epoxy) in the presence of silica. The same features from both silica and block copolymer toughening mechanisms are also present on the adhesive failure surfaces.

Ultimately, this work shows that nanoscale and micron-scale silica particles with and without functionalization can be effective in improving bulk fracture toughness and modulus, while maintaining the adhesion strength of block copolymer-modified epoxies. These promising findings may provide the foundation for further exploration of other particle additives, including functional particles that may alter other properties, in block copolymer-modified epoxies.

■ ASSOCIATED CONTENT

Supporting Information

The Supporting Information is available free of charge at https://pubs.acs.org/doi/10.1021/acsapm.2c00948.

Microsilica particle size distribution, mechanical test specimen geometries, tensile test stress versus strain curves, compact tension load versus displacement curves, bulk tensile results, single-lap-joint shear test shear stress versus displacement curves, adhesion strength results, and pictures of adhesive failure surfaces (PDF)

■ AUTHOR INFORMATION

Corresponding Authors

Frank S. Bates − *Department of Chemical Engineering and Materials Science, University of Minnesota, Minneapolis, Minnesota 55455, United States;* orcid.org/0000-0003-3977-1278; Email: bates001@umn.edu

Lorraine F. Francis − *Department of Chemical Engineering and Materials Science, University of Minnesota, Minneapolis, Minnesota 55455, United States;* orcid.org/0000-0003-2516-2957; Email: lfrancis@umn.edu

Authors

Vincent Pang − *Department of Chemical Engineering and Materials Science, University of Minnesota, Minneapolis, Minnesota 55455, United States;* orcid.org/0000-0001-5948-3543

Zachary J. Thompson − *3M Company, 3M Center, Maplewood, Minnesota 55144, United States;* orcid.org/0000-0003-3849-5638

Guy D. Joly − *3M Company, 3M Center, Maplewood, Minnesota 55144, United States*

Complete contact information is available at: https://pubs.acs.org/10.1021/acsapm.2c00948

Notes

The authors declare no competing financial interest.

■ ACKNOWLEDGMENTS

This work was funded and supported by the 3M Company. V.P. acknowledges support from the 3M Science and Technology Fellowship. Parts of this work were carried out in the Characterization Facility, University of Minnesota, which receives partial support from the NSF through the MRSEC program.

■ REFERENCES

(1) Kinloch, A. J. Toughening Epoxy Adhesives to Meet Today ' s Challenges. *MRS Bull.* **2003**, *28*, 445−448.

(2) Kinloch, A. J. *Adhesion and Adhesives*; Springer Science+Business Media LLC: New York, 1987.

(3) Hartshorn, S. R. *Structural Adhesives: Chemistry and Technology*; Plenum Press: New York, 1986.

(4) Unnikrishnan, K. P.; Thachil, E. T. Toughening of Epoxy Resins. *Des. Monomers Polym.* **2006**, *9*, 129−152.

(5) Bagheri, R.; Marouf, B. T.; Pearson, R. A. Rubber-Toughened Epoxies: A Critical Review. *Polym. Rev.* **2009**, *49*, 201−225.

(6) Kinloch, A. J.; Shaw, S. J.; Tod, D. A.; Hunston, D. L. Deformation and Fracture Behaviour of a Rubber-Toughened Epoxy: 1. Microstructure and Fracture Studies. *Polymer* **1983**, *24*, 1341−1354.

(7) Yee, A. F.; Pearson, R. A. Toughening Mechanisms in Elastomer-Modified Epoxies - Part 1 Mechanical Studies. *J. Mater. Sci.* **1986**, *21*, 2462−2474.

(8) Kin Loch, A. J.; Shaw, S. J. The Fracture Resistance of a Toughened Epoxy Adhesive. *J. Adhes.* **1981**, *12*, 59−77.

(9) Marouf, B. T.; Mai, Y.-W.; Bagheri, R.; Pearson, R. A. Toughening of Epoxy Nanocomposites: Nano and Hybrid Effects. *Polym. Rev.* **2016**, *56*, 70−112.

(10) Spitalsky, Z.; Tasis, D.; Papagelis, K.; Galiotis, C. Carbon Nanotube-Polymer Composites: Chemistry, Processing, Mechanical and Electrical Properties. *Prog. Polym. Sci.* **2010**, *35*, 357−401.

(11) Byrne, M. T.; Gun'ko, Y. K. Recent Advances in Research on Carbon Nanotube - Polymer Composites. *Adv. Mater.* **2010**, *22*, 1672−1688.

(12) Zerda, A. S.; Lesser, A. J. Intercalated Clay Nanocomposites: Morphology, Mechanics, and Fracture Behavior. *J. Polym. Sci., Part B: Polym. Phys.* **2001**, *39*, 1137−1146.

(13) Fu, S.-Y.; Feng, X.-Q.; Lauke, B.; Mai, Y.-W. Effects of Particle Size, Particle/Matrix Interface Adhesion and Particle Loading on Mechanical Properties of Particulate−Polymer Composites. *Composites, Part B* **2008**, *39*, 933−961.

(14) Qi, B.; Zhang, Q. X.; Bannister, M.; Mai, Y.-W. Investigation of the Mechanical Properties of DGEBA-Based Epoxy Resin with Nanoclay Additives. *Compos. Struct.* **2006**, *75*, 514−519.

(15) Wang, K.; Chen, L.; Wu, J.; Toh, M. L.; He, C.; Yee, A. F. Epoxy Nanocomposites with Highly Exfoliated Clay: Mechanical Properties and Fracture Mechanisms. *Macromolecules* **2005**, *38*, 788−800.

(16) Rafiee, M. A.; Rafiee, J.; Srivastava, I.; Wang, Z.; Song, H.; Yu, Z. Z.; Koratkar, N. Fracture and Fatigue in Graphene Nanocomposites. *Small* **2010**, *6*, 179−183.

(17) Johnsen, B. B.; Kinloch, A. J.; Mohammed, R. D.; Taylor, A. C.; Sprenger, S. Toughening Mechanisms of Nanoparticle-Modified Epoxy Polymers. *Polymer* **2007**, *48*, 530−541.
(18) Dibenedetto, A. T.; Wambach, A. D. The Fracture Toughness of Epoxy-Glass Bead Composites. *Int. J. Polym. Mater. Polym. Biomater.* **1972**, *1*, 159−173.
(19) Pang, V.; Thompson, Z. J.; Joly, G. D.; Bates, F. S.; Francis, L. F. Adhesion Strength of Block Copolymer Toughened Epoxy on Aluminum. *ACS Appl. Polym. Mater.* **2020**, *2*, 464−474.
(20) Li, T.; Heinzer, M. J.; Francis, L. F.; Bates, F. S. Engineering Superior Toughness in Commercially Viable Block Copolymer Modified Epoxy Resin. *J. Polym. Sci., Part B: Polym. Phys.* **2016**, *54*, 189−204.
(21) Li, L.; Zheng, S. Mechanical Properties of Epoxy/Block Copolymer Blends. In *Handbook of Epoxy Blends*; Parameswaranpillai, J., Hameed, N., Pionteck, J., Woo, E. M., Eds.; Springer International Publishing: Cham, 2015, pp 1−29.
(22) Dean, J. M.; Lipic, P. M.; Grubbs, R. B.; Cook, R. F.; Bates, F. S. Micellar Structure and Mechanical Properties of Block Copolymer-Modified Epoxies. *J. Polym. Sci., Part B: Polym. Phys.* **2001**, *39*, 2996−3010.
(23) Gerard, P.; Boupat, N. P.; Fine, T.; Gervat, L.; Pascault, J.-P. Toughness Properties of Lightly Crosslinked Epoxies Using Block Copolymers. *Macromol. Symp.* **2007**, *256*, 55−64.
(24) Thio, Y. S.; Wu, J.; Bates, F. S. Epoxy Toughening Using Low Molecular Weight Poly(Hexylene Oxide)−Poly(Ethylene Oxide) Diblock Copolymers. *Macromolecules* **2006**, *39*, 7187−7189.
(25) Liu, J.; Sue, H.-J.; Thompson, Z. J.; Bates, F. S.; Dettloff, M.; Jacob, G.; Verghese, N.; Pham, H. Strain Rate Effect on Toughening of Nano-Sized PEP−PEO Block Copolymer Modified Epoxy. *Acta Mater.* **2009**, *57*, 2691−2701.
(26) Nian, F.; Ou, J.; Yong, Q.; Zhao, Y.; Pang, H.; Liao, B. Reactive Block Copolymers for the Toughening of Epoxies: Effect of Nanostructured Morphology and Reactivity. *J. Macromol. Sci., Part A: Pure Appl.Chem.* **2018**, *55*, 533−543.
(27) Thompson, Z. J.; Hillmyer, M. A.; Liu, J.; Sue, H.-J.; Dettloff, M.; Bates, F. S. Block Copolymer Toughened Epoxy: Role of Cross-Link Density. *Macromolecules* **2009**, *42*, 2333−2335.
(28) Redline, E. M.; Declet-Perez, C.; Bates, F. S.; Francis, L. F. Effect of Block Copolymer Concentration and Core Composition on Toughening Epoxies. *Polymer* **2014**, *55*, 4172−4181.
(29) Declet-Perez, C.; Francis, L. F.; Bates, F. S. Deformation Processes in Block Copolymer Toughened Epoxies. *Macromolecules* **2015**, *48*, 3672−3684.
(30) Dean, J. M.; Verghese, N. E.; Pham, H. Q.; Bates, F. S. Nanostructure Toughened Epoxy Resins. *Macromolecules* **2003**, *36*, 9267−9270.
(31) Declet-Perez, C.; Redline, E. M.; Francis, L. F.; Bates, F. S. Role of Localized Network Damage in Block Copolymer Toughened Epoxies. *ACS Macro Lett.* **2012**, *1*, 338−342.
(32) Bucknall, C. B.; Paul, D. R. Notched Impact Behavior of Polymer Blends: Part 1: New Model for Particle Size Dependence. *Polymer* **2009**, *50*, 5539−5548.
(33) Liu, J.; Sue, H.-J.; Thompson, Z. J.; Bates, F. S.; Dettloff, M.; Jacob, G.; Verghese, N.; Pham, H. Nanocavitation in Self-Assembled Amphiphilic Block Copolymer-Modified Epoxy. *Macromolecules* **2008**, *41*, 7616−7624.
(34) Bucknall, C. B.; Paul, D. R. Notched Impact Behaviour of Polymer Blends: Part 2: Dependence of Critical Particle Size on Rubber Particle Volume Fraction. *Polymer* **2013**, *54*, 320−329.
(35) Kinloch, A. J.; Mohammed, R. D.; Taylor, A. C.; Eger, C.; Sprenger, S.; Egan, D. The Effect of Silica Nano Particles and Rubber Particles on the Toughness of Multiphase Thermosetting Epoxy Polymers. *J. Mater. Sci.* **2005**, *40*, 5083−5086.
(36) Liang, Y. L.; Pearson, R. A. The Toughening Mechanism in Hybrid Epoxy-Silica-Rubber Nanocomposites (HESRNs). *Polymer* **2010**, *51*, 4880−4890.
(37) Li, T.; He, S.; Stein, A.; Francis, L. F.; Bates, F. S. Synergistic Toughening of Epoxy Modified by Graphene and Block Copolymer Micelles. *Macromolecules* **2016**, *49*, 9507−9520.
(38) Liang, Y. L.; Pearson, R. A. Toughening Mechanisms in Epoxy-Silica Nanocomposites (ESNs). *Polymer* **2009**, *50*, 4895−4905.
(39) Liu, H.-Y.; Wang, G.-T.; Mai, Y.-W.; Zeng, Y. On Fracture Toughness of Nano-Particle Modified Epoxy. *Composites, Part B* **2011**, *42*, 2170−2175.
(40) Quan, D.; Pearson, R. A.; Ivankovic, A. Interaction of Toughening Mechanisms in Ternary Nanocomposites. *Polym. Compos.* **2018**, *39*, 3482−3496.
(41) Labak, A. *Fracture Behavior of Silica- and Rubber- Nanoparticle-Toughed Epoxies*; Lehigh University, 2015.
(42) Pang, V.; Thompson, Z. J.; Joly, G. D.; Francis, L. F.; Bates, F. S. Block Copolymer and Nanosilica-Modified Epoxy Nanocomposites. *ACS Appl. Polym. Mater.* **2021**, *3*, 4156−4167.
(43) Zhou, H.; Liu, H.-Y.; Zhou, H.; Zhang, Y.; Gao, X.; Mai, Y.-W. On Adhesive Properties of Nano-Silica/Epoxy Bonded Single-Lap Joints. *Mater. Des.* **2016**, *95*, 212−218.
(44) Jouyandeh, M.; Moini Jazani, O.; Navarchian, A. H.; Saeb, M. R. High-Performance Epoxy-Based Adhesives Reinforced with Alumina and Silica for Carbon Fiber Composite/Steel Bonded Joints. *J. Reinf. Plast. Compos.* **2016**, *35*, 1685−1695.
(45) Dodiuk, H.; Kenig, S.; Blinsky, I.; Dotan, A.; Buchman, A. Nanotailoring of Epoxy Adhesives by Polyhedral-Oligomeric-Sil-Sesquioxanes (POSS). *Int. J. Adhes. Adhes.* **2005**, *25*, 211−218.
(46) Kar, S.; Gupta, D.; Banthia, A. K. Effect of Aluminum Silicate on the Impact and Adhesive Properties of Toughened Epoxy Resins. *J. Adhes. Sci. Technol.* **2002**, *16*, 1901−1914.
(47) Kinloch, A. J.; Lee, J. H.; Taylor, A. C.; Sprenger, S.; Eger, C.; Egan, D. Toughening Structural Adhesives via Nano- and Micro-Phase Inclusions. *J. Adhes.* **2003**, *79*, 867−873.
(48) Fallahi, M.; Moini Jazani, O.; Molla-Abbasi, P. Design and Characterization of High-performance Epoxy Adhesive with Block Copolymer and Alumina Nanoparticles in Aluminum-aluminum Bonded Joints: Mechanical Properties, Lap Shear Strength, and Thermal Stability. *Polym. Compos.* **2022**, *43*, 1637−1655.
(49) Burton, B.; Alexander, D.; Klein, H.; Garibay-Vasquez, A.; Pekarik, A.; Henkee, C.. *Epoxy Formulations Using Jeffamine® Polyetheramines*. Huntsman Corp, 2005, Vol. *4*−*13*.
(50) ASTM International. ASTM D638-14 Standard Test Method for Tensile Properties of Plastics; *ASTM Book of Standards*; ASTM International: West Conshohocken, PA, 2014, pp 1−17.
(51) ASTM International. ASTM D5045-14 Standard Test Methods for Plane-Strain Fracture Toughness and Strain Energy Release Rate of Plastic Materials. *ASTM Book of Standards*; ASTM International: West Conshohocken, PA, 2014, pp 1−9.
(52) ASTM International. ASTM D1002-10(2019) Standard Test Method for Apparent Shear Strength of Single-Lap-Joint Adhesively Bonded Metal Specimens by Tension Loading (Metal-to-Metal). *ASTM Book of Standards*; ASTM International: West Conshohocken, PA, 2019, pp 1−5.
(53) da Silva, L. F. M.; Rodrigues, T. N. S. S.; Figueiredo, M. A. V.; de Moura, M. F. S. F.; Chousal, J. A. G. Effect of Adhesive Type and Thickness on the Lap Shear Strength. *J. Adhes.* **2006**, *82*, 1091−1115.
(54) Callister, W. D.; Rethwisch, D. G. *Materials Science and Engineering - An Introduction*, 9th ed.; Sayre, D., Ed.; John Wiley & Sons, Inc: Hoboken, NJ, 2014.
(55) Chu, X. L.; Nikolov, A. D.; Wasan, D. T. Effects of Particle Size and Polydispersity on the Depletion and Structural Forces in Colloidal Dispersions. *Langmuir* **1996**, *12*, 5004−5010.
(56) Crocker, J. C.; Matteo, J. A.; Dinsmore, A. D.; Yodh, A. G. Entropic Attraction and Repulsion in Binary Colloids Probed with a Line Optical Tweezer. *Phys. Rev. Lett.* **1999**, *82*, 4352−4355.
(57) Likos, C. N. Effective Interactions in Soft Condensed Matter Physics. *Phys. Rep.* **2001**, *348*, 267−439.
(58) James, G. K.; Walz, J. Y. Experimental Investigation of the Effects of Ionic Micelles on Colloidal Stability. *J. Colloid Interface Sci.* **2014**, *418*, 283−291.

https://doi.org/10.1021/acsapm.2c00948
ACS Appl. Polym. Mater. 2022, 4, 6169−6178

(59) Richetti, P.; Kékicheff, P. Direct Measurement of Depletion and Structural Forces in a Micellar System. *Phys. Rev. Lett.* **1992**, *68*, 1951−1954.
(60) Grillet, A. C.; Galy, J.; Gérard, J. F.; Pascault, J. P. Mechanical and Viscoelastic Properties of Epoxy Networks Cured with Aromatic Diamines. *Polymer* **1991**, *32*, 1885−1891.
(61) Dittanet, P.; Pearson, R. A. Effect of Silica Nanoparticle Size on Toughening Mechanisms of Filled Epoxy. *Polymer* **2012**, *53*, 1890−1905.
(62) Mori, T.; Tanaka, K. Average Stress in Matrix and Average Elastic Energy of Materials with Misfitting Inclusions. *Acta Metall.* **1973**, *21*, 571−574.
(63) Spanoudakis, J.; Young, R. J. Crack Propagation in a Glass Particle-Filled Epoxy Resin. *J. Mater. Sci.* **1984**, *19*, 473−486.
(64) Wetzel, B.; Rosso, P.; Haupert, F.; Friedrich, K. Epoxy Nanocomposites − Fracture and Toughening Mechanisms. *Eng. Fract. Mech.* **2006**, *73*, 2375−2398.
(65) Declet-Perez, C.; Francis, L. F.; Bates, F. S. Cavitation in Block Copolymer Modified Epoxy Revealed by In Situ Small-Angle X-Ray Scattering. *ACS Macro Lett.* **2013**, *2*, 939−943.
(66) Tsai, M. Y.; Oplinger, D. W.; Morton, J. Improved Theoretical Solutions for Adhesive Lap Joints. *Int. J. Solids Struct.* **1998**, *35*, 1163−1185.
(67) Kim, W. S.; Yun, I. H.; Lee, J. J.; Jung, H. T. Evaluation of Mechanical Interlock Effect on Adhesion Strength of Polymer-Metal Interfaces Using Micro-Patterned Surface Topography. *Int. J. Adhes. Adhes.* **2010**, *30*, 408−417.
(68) Jennings, C. W. Surface Roughness and Bond Strength of Adhesives. *J. Adhes.* **1972**, *4*, 25−38.

https://doi.org/10.1021/acsapm.2c00948
ACS Appl. Polym. Mater. 2022, 4, 6169−6178